Anisotropic Two-Dimensional Friedel Oscillations

Ph. Hofmann,[1] B. G. Briner,[2] M. Doering,[2] H.-P. Rust,[2] E. W. Plummer,[1] and A. M. Bradshaw[2]
[1]*Department of Physics and Astronomy, The University of Tennessee, Knoxville, Tennessee 37996 and Oak Ridge National Laboratories, Oak Ridge, Tennessee 37831-6057*
[2]*Fritz-Haber-Institut der Max-Planck-Gesellschaft, Faradayweg 4-6, 14195 Berlin, Germany*
(Received 13 December 1996)

Scanning tunneling microscopy at 4 K shows highly anisotropic screening charge density oscillations on Be(10$\bar{1}$0) in the vicinity of surface defects and steps. The forms of these oscillations, which derive from the Friedel oscillations, can be directly related to the two-dimensional band structure of the surface (two electron pockets at the boundary of the surface Brillouin zone). Simple calculations show that the Friedel oscillations in such a case will contain major contributions from wavelengths which do not correspond to any Fermi wave vector. [S0031-9007(97)03550-3]

PACS numbers: 73.20.At, 71.18.+y, 71.20.Dg, 72.10.Fk

Nearly forty years ago, Friedel showed that the screening of a charged point impurity in a simple metal results in long-range modulations in the charge density caused by the abrupt change in the density of states at the Fermi energy E_F [1]. The wavelength of these modulations is given by $2\pi/2k_F$, k_F being the wave vector of the electrons at the Fermi level. In metals these Friedel oscillations are the primary mechanism for long range interactions. Essentially the same mechanism was invoked four years earlier by Ruderman and Kittel to describe the magnetic interaction between two nuclei in a simple metal. In that case, however, the scattering is caused by the hyperfine interaction between the nuclei and the conduction electrons [2]. Only a few theoretical papers deal with Friedel oscillations from a nonspherical Fermi surface [3–5], even though it is precisely these types of materials which are relevant for magnetism. Experimentally, it is difficult to access directly Friedel oscillations in the bulk. On surfaces, however, two-dimensional modulations of the charge density can be investigated by means of scanning tunneling microscopy (STM) [6–9]. In this Letter we report STM results from the Be(10$\bar{1}$0) surface which clearly demonstrate the existence of anisotropic screening waves as a consequence of a noncircular Fermi line. We show theoretically that in such a case periodicities in the Friedel oscillations may be found which are not associated with any Fermi wave vector.

Previous STM results by several groups have shown standing wavelike patterns in the vicinity of steps and defects on the close-packed surfaces of Cu, Au, and Be [6–8]. The standing waves were interpreted as resulting from surface state electrons scattered by the defects, i.e., in terms of Friedel oscillations. On all three surfaces, the surface state has a similar shape: It is free electronlike with a circular Fermi line around the center of the surface Brillouin zone (SBZ). This leads to isotropic screening and to, for instance, circular wave fronts around a point defect. Indeed, in the case of Be(0001) Sprunger *et al.* have shown that Fourier-transformed low-bias STM images show a circle of radius $2k_F$ which essentially represents the Fermi line and allows the precise determination of the Fermi wave vector [8].

The unusual electronic structure of the Be(10$\bar{1}$0) surface [10] offers an ideal possibility for testing the effect of a noncircular Fermi line on the Friedel oscillations. In the bulk, Beryllium is a simple metal with unusual electronic properties: The bonding is highly directional and the density of electronic states (DOS) shows a minimum in the vicinity of E_F. The (0001) and (10$\bar{1}$0) surfaces of Be still, however, have a high DOS at E_F due to the existence of surface states, such that the surface region may be viewed as a quasi-two-dimensional metal. The shape of the surface state Fermi line on Be(0001) and Be(10$\bar{1}$0) is very different: While it is a circle around the zone center on Be(0001) [11,12], it is given by an elliptical electron pocket around the $\bar{A}$ point of the SBZ on Be(10$\bar{1}$0) (see Fig. 1) [10]. The bottom of the electron pocket band is at $E_0 = -320$ meV and the dispersion around $\bar{A}$ is almost parabolic ($m^*/m_0 \cong 0.5$–1.2).

The expectation that a Fermi line like the one in Fig. 1 should lead to pronounced anisotropic screening is

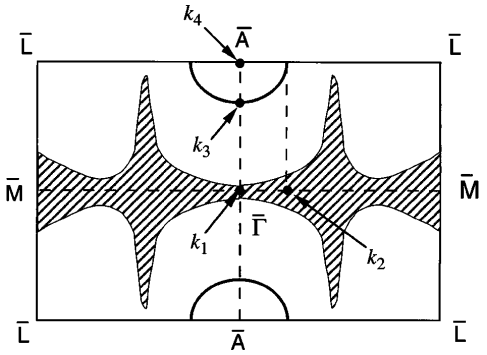

FIG. 1. The first Brillouin zone and Fermi line of Be(10$\bar{1}$0) after Ref. [10]. The thick lines represent the contribution of the surface state, the shaded region is the projection of the bulk Fermi surface (qualitatively after Ref. [21]). The density of states at E_F is much higher for the surface state than for the total bulk contribution. The significance of the points k_1, k_2, k_3, and k_4 is explained in the text.

confirmed by the experiment. Figure 2(a) shows an 155 Å × 155 Å STM topograph taken at a bias voltage of −50 mV on the sample (i.e., with the electrons from the sample tunneling into empty tip states) and a constant tunneling current of 100 pA. The data were taken with an Eigler-type STM operating in UHV at a temperature of 4 K [13,14]. The crystal was cleaned using standard procedures described elsewhere [10,15,16]. A double-atomic step is meandering through the middle of the image. In the upper right corner a regular, rowlike pattern is clearly visible and corresponds to the close-packed atom rows on this surface (see inset) [15]. In the vicinity of the steps, however, this regular pattern is severely distorted: Originating from the steps in the $\overline{\Gamma}\,\overline{M}$ direction a wavelike pattern can be seen, which we interpret as a superposition of the actual standing electron waves and the lattice rows. No waves or only very weak waves, however, are found at steps in the $\overline{\Gamma}\,\overline{A}$ direction. A detailed analysis of the voltage and current dependence will be presented elsewhere [16].

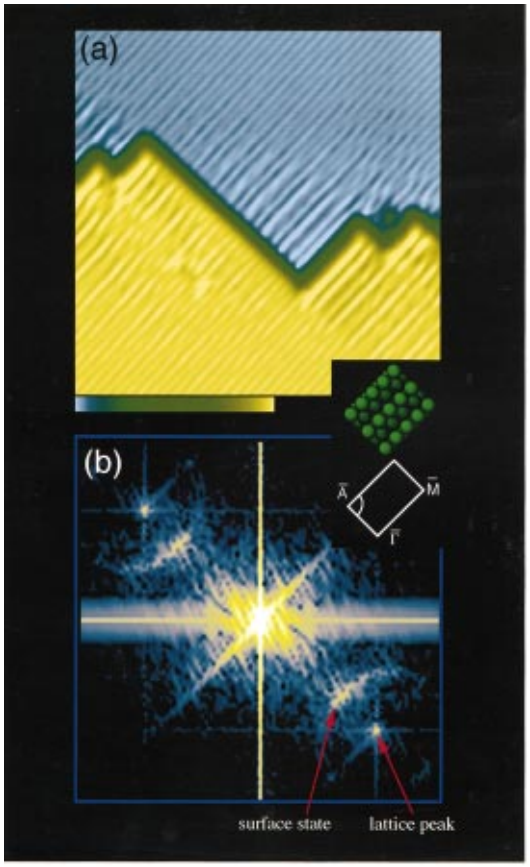

FIG. 2(color). (a) A 155 Å × 155 Å STM topograph taken at a bias voltage of −50 mV on the sample and a tunneling current of 100 pA. The line in the middle of the image is a double-atomic step. The color bar on the bottom of the images gives the z scale. The total range is the step height +0.2 Å = 2.08 Å. (b) Logarithm of the power spectrum of the image (3.92 $Å^{-1}$ × 3.92 $Å^{-1}$). The points in the $\overline{\Gamma}\,\overline{A}$ direction correspond to the lattice periodicity of 3.58 Å. The elliptically shaped features around these points originate from the Fermi line. The inset shows a real space top view of the surface as well as the irreducible part of the SBZ with the Fermi line.

A Fourier-transformed image (FT), i.e., the logarithm of the power spectrum of Fig. 2(a), is shown in Fig. 2(b). The points marked "lattice peaks" calibrate the image since they are the reciprocal lattice vector positions in the $\overline{\Gamma}\,\overline{M}$ direction caused by the distance between the lattice rows visible in the image. The two half-elliptical features around the reciprocal lattice peaks labeled "surface state" are dictated by the Fermi line in Fig. 1 [8]; their distance from the origin is, however, not k_F, but $2k_F$ due to the fact that we observe waves on the charge density rather than in the actual wave functions. The Fermi level crossings derived from our data are consistent with the photoemission results of Ref. [10]. The intensity of the elliptical features has a maximum on the $\overline{\Gamma}\,\overline{A}$ line. Indeed, if there were only a single step in the $\overline{\Gamma}\,\overline{M}$ direction, symmetry would dictate that only a dot on the $\overline{\Gamma}\,\overline{A}$ line would appear in the FT. The fact that we observe the rest of the half ellipse is due to scattering of electrons from kinks and defects. If we consider the intensity distribution on the $\overline{\Gamma}\,\overline{A}$ line it is clear that what we see in the real space image in this direction is, in fact, a superposition of mainly two wavelengths: the surface state and the lattice peak. The three strong lines through the origin are caused by the sharp cutoff of the image at the edges and the main step direction. The latter probably also causes the weak lines in the FT running through the reciprocal lattice points parallel to the $\overline{\Gamma}\,\overline{M}$ direction.

It is important to realize that an STM image does not give a straightforward access to the actual Friedel oscillations, i.e., the modulations in the total charge density. The tunneling current I is given by an integral over the energy-dependent local density of states (LDOS) multiplied by a barrier factor for the tunneling [17,18]. Hence, an STM topograph taken in the constant current mode gives a distorted image of the Friedel oscillations, provided that the tunneling voltage is greater than the width of the surface state band. At a smaller tunneling voltage a weighted image on the energy resolved Friedel oscillations is taken. In the case of a very small tunneling voltage and a pointlike tip, I is *directly* proportional to the LDOS at the Fermi level and the images provide quantitative information about the oscillations associated with the electrons at E_F.

The main physical concepts underlying the anisotropic screening can be elucidated by generalizing a simple model already used for Cu(111) and Au(111) [6,19] where the density of states in the vicinity of a hard-wall step is calculated. The surface state wave function is given by a Bloch wave:

$$\psi_k = Ce^{i\mathbf{k}r}e^{-\kappa(\mathbf{k})z}u(\mathbf{r}), \qquad (1)$$

where $\mathbf{r} = (x, y, 0)$, $\mathbf{k} = (k_x, k_y, 0)$. $\kappa(\mathbf{k})$ describes the decay of the wave functions into the vacuum. $u(\mathbf{r})$ is a

lattice periodic function. For the purpose of demonstrating just the qualitative effects of a noncircular Fermi line, we focus on the free electron part of the wave functions in the surface plane and disregard $\exp[-\kappa(\mathbf{k})z]u(\mathbf{r})$ as well as any tip effects. The implications of the Bloch nature of the wave functions on the detailed shape of the standing electron waves will be discussed elsewhere [20].

A step on the surface is modeled [6,19] as an infinitely long hard wall in the x direction which imposes a boundary condition on the wave functions and leads to

$$\psi_k = C \sin(k_y y) e^{i\mathbf{k}_x x}. \tag{2}$$

The total electron density at a distance y from the step is given by

$$\rho(y) \propto \int_{E=E_0}^{E_F} |\psi_\mathbf{k}|^2 \, dE = \int_A |\psi_\mathbf{k}|^2 \, d\mathbf{k} = \int_A \sin^2 y k_y \, d\mathbf{k} \, . \tag{3}$$

E_0 is the bottom of the surface state band and A is the area inside the Fermi line. A step in the y direction gives an analogous result. Note that this integral represents the total charge density which includes the Friedel oscillation. In the case of a circular Fermi line around the zone center the k_y integration extends from zero (because sine-squared is an even function) to k_F. The cutoff at k_F results in the Friedel oscillations. The k_x integration has merely a scaling effect. For a general Fermi line, however, the lower k_y limit need not be zero and we might expect additional oscillations associated with this new cutoff. Yet another cutoff can be caused by a tunneling voltage V smaller than the band width E_0 of the surface state so that $\rho(y, V)$ rather than $\rho(y)$ has to be calculated, since not all the states inside A contribute to the tunneling current [18].

We have simulated the experimental situation by calculating (3) for the Fermi line geometry in Fig. 1. Figure 3(a) shows the result both for steps along $\overline{\Gamma}\,\overline{A}$ (dashed line) and $\overline{\Gamma}\,\overline{M}$ (solid line). As in the image of Fig. 2, only states between -50 meV and E_F have been taken into account. Figure 3(b) shows the one-dimensional Fourier transforms of Fig. 3(a). As expected, the wavelength and shape of the oscillations are very different for the two step orientations. For a step in the $\overline{\Gamma}\,\overline{A}$ direction, i.e., perpendicular to the closed packed atom rows, ρ shows an oscillation with basically one wavelength. The corresponding peak in the FT [Fig. 3(b)] corresponds to the cutoff at the Fermi energy ($\lambda = 2\pi/2k_2$). The width of the peak is dictated by the finite tunneling voltage and the dispersion of the surface state. For the other step, the oscillation is more rapid and looks more complicated. Again, a peak in the power spectrum is found which corresponds to the cutoff at E_F ($\lambda = 2\pi/2k_3$) and to the "surface state" feature in Fig. 2(b). A second peak in the power spectrum is found at $\lambda = 2\pi/2k_4$ and corresponds to the cutoff of the integral (3) at the zone boundary. Note that the wave associated with k_4 does not have half a Fermi wavelength

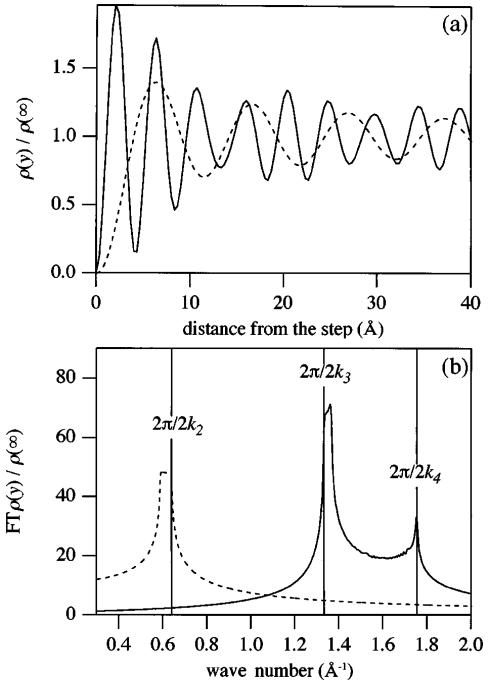

FIG. 3. (a) The density of states in the vicinity of a hard wall step on Be($10\bar{1}0$) for a step parallel to the $\overline{\Gamma}\,\overline{A}$ direction (dashed line) and the $\overline{\Gamma}\,\overline{M}$ direction (solid line). (b) The power spectrum of (a). The three wavelengths highlighted correspond to the k points in Fig. 1.

but the lattice periodicity. This leads to the complicated shape of the oscillation similar to the coupling in magnetic multilayers [5].

Our simple model enables us to understand the basic principles of the anisotropic Friedel oscillations. However, there are some obvious differences between experiment and theory: There are no, or only extremely weak, oscillations present in the $\overline{\Gamma}\,\overline{M}$ direction. This is perhaps not surprising if we keep in mind the shortcomings of the model: Firstly, the calculation is performed for the limiting case of an infinitely long step. This leads to waves at the step which runs in the $\overline{\Gamma}\,\overline{A}$ direction, even though none of the electrons have a momentum strictly perpendicular to the step. In the other limiting case of a point defect the absolute magnitude of the charge modulation in the $\overline{\Gamma}\,\overline{M}$ direction will be small. In our STM image we have a situation somewhere between these two limits. Secondly, the steps are not infinitely high and thus the reflection coefficient for the two step types may be different. Finally, the tunneling process itself has not been considered at all in the model.

In conclusion, using STM data from Be($10\bar{1}0$) at 4 K, we have shown how electron pockets at the zone boundary lead to pronounced anisotropic screening. The basic features of the STM images can be understood in terms of a simple model in which a step on the surface is represented by an infinitely long hard wall. This picture suggests that for a Fermi line which cuts the boundary

of the surface Brillouin zone, charge density oscillations can be found which do *not* correspond to any Fermi wave vector in the system. These oscillations coincide with the lattice periodicity and are therefore not accessible in the experiment. The more complicated shape and wavelength of Friedel oscillations from noncircular and nonspherical Fermi surfaces in two- and three-dimensional systems, respectively, should have important consequences for many physical phenomena.

The authors acknowledge stimulating discussions with G. D. Mahan and J. M. Carpinelli. This work was supported by the National Science Foundation under Grant No. NSF-95-10132. Ph. Hofmann thanks the Alexander v. Humboldt-Stiftung for a fellowship. Part of this study was conducted at ORNL and supported by the U.S. Department of Energy under Contract No. DE-AC05-96OR22464 with Lockheed Martin Energy Research Corp.

[1] J. Friedel, Nuovo Cimento (Suppl.) **7**, 287 (1958).
[2] M. A. Ruderman and C. Kittel, Phys. Rev. **96**, 99 (1954).
[3] L. M. Roth, H. J. Zeiger, and T. A. Kaplan, Phys. Rev. **149**, 519 (1966).
[4] G. D. Mahan, Int. J. Mod. Phys. B **9**, 1327 (1995).
[5] F. Herman and R. Schrieffer, Phys. Rev. B **46**, 5806 (1992).
[6] M. F. Crommie, C. P. Lutz, and D. M. Eigler, Nature (London) **363**, 524 (1993).
[7] Y. Hasegawa and Ph. Avouris, Phys. Rev. Lett. **71**, 1071 (1993).
[8] P. T. Sprunger, L. Petersen, E. W. Plummer, E. Lægsgaard, and F. Besenbacher, Science **275**, 1764 (1997).
[9] M. C. M. M. van der Wielen, A. J. A. van Roij, and H. van Kempen, Phys. Rev. Lett. **76**, 1075 (1996).
[10] Ph. Hofmann, R. Stumpf, V. M. Silkin, E. V. Chulkov, and E. W. Plummer, Surf. Sci. **355**, L278 (1996).
[11] R. A. Bartynski, E. Jensen, T. Gustafsson, and E. W. Plummer, Phys. Rev. B **32**, 1921 (1985).
[12] E. V. Chulkov, V. M. Silkin, and E. N. Shirykalov, Surf. Sci. **188**, 287 (1987).
[13] P. S. Weiss and D. M. Eigler in *Nanosources and Manipulation of Atoms under High fields and Temperatures*, edited by V. T. Binh *et al.*, NATO ASI, Ser. E, Vol. 235 (Kluwer Academic Publishers, Dordrecht, 1993).
[14] H.-P. Rust, J. Buisset, E. K. Schweizer, and L. Cramer, Rev. Sci. Instrum. **68**, 129 (1997).
[15] Ph. Hofmann, K. Pohl, R. Stumpf, and E. W. Plummer, Phys. Rev. B **53**, 13 715 (1996).
[16] B. G. Briner, Ph. Hofmann, M. Doering, H.-P. Rust, E. W. Plummer, and A. M. Bradshaw (to be published).
[17] J. Tersoff and D. R. Hamann, Phys. Rev. B **31**, 805 (1985).
[18] G. Hörmandinger, Phys. Rev. B **49**, 13 897 (1994).
[19] Ph. Avouris, I.-W. Lyo, R. E. Walkup, and Y. Hasegawa, J. Vac. Sci. Technol. B **12**, 1447 (1994).
[20] B. G. Briner, Ph. Hofmann, M. Doering, H.-P. Rust, E. W. Plummer, and A. M. Bradshaw, Europhys. Lett. (to be published).
[21] T. L. Loucks and P. H. Cutler, Phys. Rev. **133**, A819 (1964).